

EVALUATION OF WATER FILM BY REYNOLDS' EQUATION IN DEEP DRAWING USING HIGH-PRESSURED WATER JET

TAKASHI KUBOKI^{*}, YUKI HORIKOSHI^{*}, MAKOTO MURATA^{*}, KAZUMI MATSUI[†] AND MAKOTO TSUBOKURA[‡]

^{*} Department of Mechanical Engineering & Intelligent Systems
The University of Electro-Communications
1-5-1 Chofu Gaoka, Chofu-shi, Tokyo 182-8585, Japan
e-mail: kuboki@mce.uec.ac.jp

[†] Yokohama National University
79-1 Tokiwadai, Hodogaya-ku, Yokohama, Kanagawa 240-8501, Japan

[‡] Hokkaido University
Kita-13, Nishi-8, Kita-ku, Sapporo, Hokkaido 060-0808, Japan

Key words: Reynolds' equation, Deep drawing, Lubrication, High-pressured Water Jet.

Abstract. The authors had proposed a deep drawing method using high-pressured jet waters as lubricant. This method aimed to suppress the usage of oil or other chemical lubricants, which might require some additional processes for lubricant removal and become a nuisance in environment. The conditions had been determined through trial and error approach without knowing water behaviors as lubricant. As a result, some scars and dimples were observed on the surface of deformed cup. In the present paper, a numerical model was composed for the evaluation of the water behaviors as lubricant. Darcy-Weisbach equation was used for evaluation of pressure drop between nozzle exit and pump, while Reynolds' equation was used for the thin film of fluid between the die and blank. The data of blank deformation in FEM was considered for the determination of the thickness distribution of the fluid film. The characteristics of the water were evaluated by the composed numerical method, and the results were used for examination of lubrication characteristics in experiments.

1 INTRODUCTION

Lubricants have almost inevitably been used in cold metal working. Lubricants have effects of securing smooth movement of materials on the tool surfaces as well as of cooling down the temperature of materials and tools. There would be two types of lubrication methods in terms of supplying lubricants between materials and tools. One is the method to apply lubricants on the surfaces of materials or tools in advance of metal working, and the other is to pump lubricants with high pressure.

The first type would include rolling, forging and drawing. Some drawing processes would be an intermediate method as the material would drag liquid into the gap between the material

and die surfaces [1]. The second type would include many hydroforming processes of sheet metals and tubes.

Deep drawing is conducted by both of the two methods in the industry. It is well known that characteristics of lubricants affect the formability significantly in the first type of deep drawing [2]. The 2nd type method has recently been applied for improvement of processes and products. A method, called "hydraulic counter-pressure deep drawing" or "hydromechanical deep-drawing" is used for enhancement of the surface integrity and forming limits, or for suppression of material and die costs [3]. Numerical analyses using the Finite Element Method have been tried to clarify the effect of process parameters on the shape and defect of deep-drawn materials [4].

The authors had proposed a deep drawing method using high pressure jet waters as lubricant [5], of which the lubrication method would be categorized in the second type. This method aimed to suppress the usage of oil or other chemical lubricants, which might require some additional processes for lubricant removal and become a nuisance in environment. Even though the authors successfully deform the blank into a cup shape without conventional oil or chemical lubricants, the conditions had been determined through trial and error approach without knowing water jet behaviors. As a result, some scars and dimples had been observed on the surface of deformed cup, and there might be some other optimum process conditions. Although the authors had tried to apply computational fluid dynamics (CFD) based on Navier–Stokes equations equation for analysis of the water jet, the analysis result had become unstable at several conditions [6].

In the present paper, a numerical model was composed for the evaluation of the water behaviors as lubricant. Darcy-Weisbach equation was used for evaluation of pressure drop between nozzle exit and pump, while Reynolds' equation, instead of Navier-Stokes' [6], was used for the thin film of fluid between the die and blank. The data of blank deformation in FEM was considered for the determination of the thickness distribution of the fluid film. The characteristics of the water were evaluated by the composed numerical method, and the results were used for examination of lubrication characteristics in experiments.

2 DEEP DRAWING WITH HIGH-PRESSURED WATER JET

2.1 Experimental setup

The basic composition of experimental setup was the same as that in conventional deep drawing machine, which consists of a die, a blank holder and a punch [5]. The unique point of the proposed method is that the die had nozzles on the die shoulder as shown in Figure 1.

The nozzles were placed at every 45 degrees in the hoop direction, and their tilt angle is 45 degrees to the horizontal plane. The nozzle diameter D_n was 0.6 mm, and

pump pressure P_0 was 40 MPa according to the authors' previous research [5]. The die consisted of inner and outer dies, between which two O-rings are inserted for prevention of water leakage. The high-pressured water was supplied from the channel to the nozzles. The detailed conditions are shown in Table 1.

Table 2 shows mechanical properties for the aluminium 1100. The stress-strain diagram was obtained from tension test. These values of stress and strain were used for finite element analysis. The stress and strain relationship after uniform elongation was calculated by

extrapolation. Commonly used elastic constants of aluminium were selected for Young's modulus E and Poisson's ratio ν .

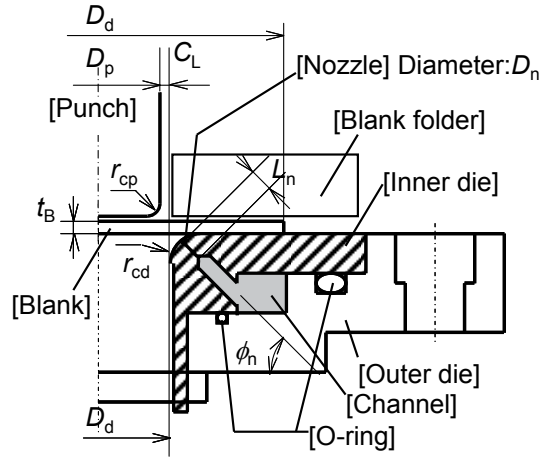


Figure 1: Composition of experimental setup with nozzles for high pressured water jet

Table 1: Deep drawing conditions

Working condition	Pump pressure P_0 /MPa.	40
	Blank holding force F_h /kN	3
	Clearance C_L /kN	1.15
Punch	Diameter D_p /mm	30
	Corner radius R_{cp} /mm	2.5
Die	Inner diameter D_d /mm	32.3
	Corner radius R_{cd} /mm	5.0
Nozzle	Diameter D_n /mm	0.6
	Length L_n /mm	10
	Tilt angle ϕ /degrees	45
Blank	Thickness t_0 /mm	1.0
	Diameter D_b /mm	60

Table 2: Mechanical properties of aluminium 1100

Elastic properties	Young's Modulus E /MPa	72000				
	Poisson's ratio ν	0.33				
Plastic strain	0.0	0.02	0.04	0.06	0.08	
Uni-axial stress	89	108	109	109	109	

2.2 Experimental results

The blank was successfully deformed into a cup shape as shown in Figure 2. Deformed shapes are shown in the middle of process at the stroke S of 3.7, 8.2, 16.3 mm and at the end. The wall height increased with increase of stroke S as the conventional deep drawing. However, some dimples were observed and it seemed to be stamped at the early stage of deep drawing. The dimples were denoted with black marker in Figure 2(e) and (f).



(a) $S=3.7\text{mm}$ (b) $S=8.2\text{mm}$ (c) $S=16.3\text{mm}$ (d) End (e) Dimples at $S=10\text{mm}$ (f) Dimples at the end

Figure 2: Deformed shape at each stroke S

3 NUMERICAL ANALYSES

3.1 Combination of numerical analyses

The FEM was carried out to obtain the deformation of material, which was used for the CFD based on Reynolds' equation for calculating the fluid condition between the die and material. Another theoretical examination was carried for the evaluation of nozzles in the die.

3.2 FEM model for blank deformation

Elastic-plastic analysis was carried out using the commercial code ELFEN, which was developed by Rockfield Software Limited, Swansea. An implicit scheme was used and a von Mises' yield criterion was adopted, and the normality principle was applied to the flow rule. Constraints were dealt with by the penalty function method. The analysis was carried out in axisymmetric way, and a quadrilateral element was used because of the simplicity of the material deformation. The F-bar method was applied to the element for overcoming volumetric locking with simple quadrilateral elements [7].

Table 3: Conditions for FE analysis

Friction coefficient μ		0.15 for blank holder side 0.08 for die side
Mesh division	Thickness Radius	0.25 mm / div 0.28 mm/div.
Analysis scheme		2D static implicit
Element type		Quadrilateral

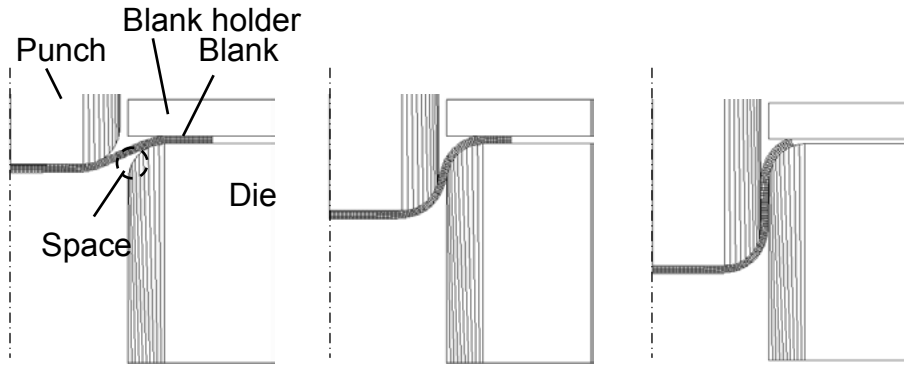


Figure 3: Deformation in FE analysis

Table 3 shows conditions for finite element analysis. An example of FEM model is shown in Figure 3. The material is certainly pushed into the die-hole attendant upon the stroke increase.

3.3 Theoretical examination of nozzle

Although both of the nozzles and water film between the die and material could be resumed in a CFD, it might be complicated to compose model and lead to instability in analysis. Here, the nozzle with diameter D_n and length L_n was examined theoretically as follows.

- (1) Assume surface roughness e [m] at the nozzle surface.
- (2) Assume pressure at the nozzle exit P_1 [Pa] and calculate the pressure drop $\Delta P = P_1 - P_0$.
- (3) Calculate approximate flow velocity u_m [m·s⁻¹] inside the nozzle using Bernoulli equation from ΔP .
- (4) Calculate Reynolds number R_e from u_m .
- (5) Calculate friction f at the nozzle from R_e and surface roughness e using Swamee-Jain equation [8].
- (6) Calculate the pressure velocity u_m from using inverse function of Darcy-Weisbach equation [9] as follows:

$$u_m = \sqrt{\frac{2\Delta P}{\rho}} \sqrt{\frac{1}{4f} \frac{D_n}{L_n}} \quad (1)$$

where ρ = density of the fluid.

- (7) Iterate (4) to (6) until velocity u_m becomes stable.
- (8) As a result, and u will be calculated as a function of surface roughness e and pressure at the nozzle exit P_1 .

Swamee-Jain equation, which is an equation for turbulent fluid, was used because Reynolds number R_e was large enough at 1.45×10^5 when the nozzle exit was under atmospheric pressure. The roughness e would be identified by measuring the water flow volume, which came out from the nozzle under the atmosphere pressure in advance.

The result of identification is shown in Figure 4. The roughness was identified as $40\ \mu\text{m}$ by comparing with the theoretical and experimental results when P_1 was atmospheric pressure. This figure explains the basic characteristics of a nozzle. When the pressure at the nozzle exit P_1 is equal to the pump pressure $P_0 = 40\ \text{MPa}$, flow velocity inside the nozzle u_m becomes zero. When the exit pressure P_1 is zero, the flow velocity u_m becomes maximum. The flow velocity u increases with decrease of surface roughness e .

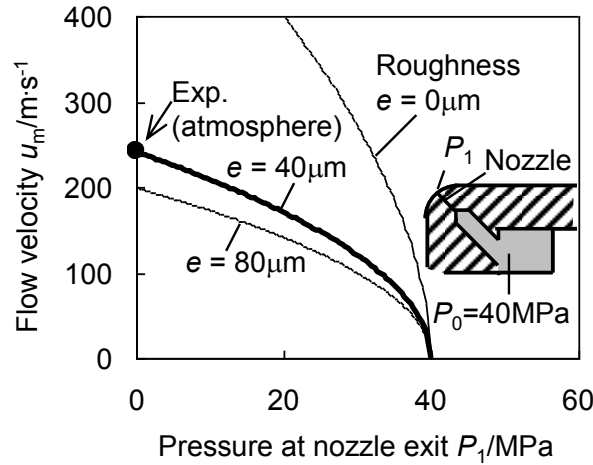


Figure 4: Identification of roughness inside nozzle based on theories of Darcy-Weisbach and Swamee-Jain equations.

3.4 Computational fluid dynamics for water film based on Reynolds equation

The fluid flow in the water film between die and material was calculated by CFD for the each progress of deep drawing, using software based on Reynolds equation. The main part of software was developed by Firmflow Co., Ltd. in Japan and customized by the authors. The finite difference method was applied assuming the following equations for the thin water film [10]:

$$\frac{\partial}{\partial x} \left(t_w^3 \frac{\partial p}{\partial x} \right) + \frac{\partial}{\partial y} \left(t_w^3 \frac{\partial p}{\partial y} \right) = 6\mu_c \left\{ (U_1 - U_2) \frac{\partial t_w}{\partial x} + \frac{\partial}{\partial x} (U_1 + U_2) + 2V_2 \right\} \quad (2)$$

where t_w is water thickness [m], p is pressure [Pa], x is latitude position [m], y is meridian position [m], μ_c is viscosity coefficient [Pa·s], U_1 is surface velocity of the die [$\text{m}\cdot\text{s}^{-1}$], U_2 is surface velocity of the blank [$\text{m}\cdot\text{s}^{-1}$] and V_2 is relative velocity of the blank to the die in normal direction to the die surface. The first, second and third terms of the right-hand side are known as the effects of wedge, contraction and squeeze, respectively. Hereby, the second and third term were neglected.

Besides the Reynolds' equation for the thin water film, the following assumptions were made:

- (1) The fluid becomes stable against the plastic deformation. Therefore, CFD was conducted for the individual progresses of the FEM for plastic deformation.

- (2) The material deforms in axisymmetric way. The analysed 2D geometries of lower surface of the material are unfolded in the hoop direction for the determination of upper boundary of the water film.
- (3) The lower surface of the material would be displaced according to the pressure amount, and the gap between the material lower and the die upper surfaces was defined as uplift Δz as shown in Figure 5.
- (4) Uplift Δz is constant during deep drawing.
- (5) The fluid follows the Reynolds' equation, neglecting the effect of turbulent flow.

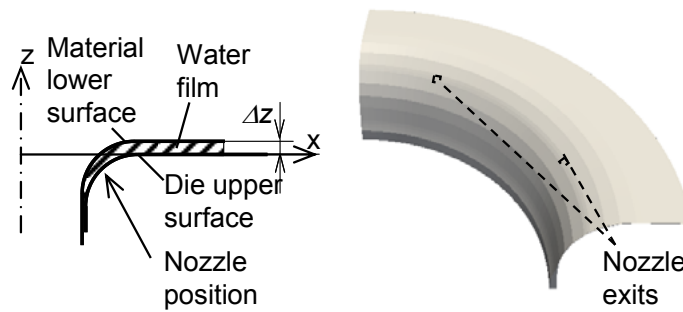


Figure 5: Model of water film in CFD and the definition of uplift Δz

The analysis was conducted in a quarter models considering the symmetry as shown in Figure 5. The pressure was given on the nozzle exit, which had a rectangle shape instead of a circle, but had the same area as the actual nozzle used in the experiment. Other conditions are shown in Table 4.

Table 4: Conditions for CFD analysis

Viscosity coefficient μ_C / Pa·s		0.001
Division	Thickness	3 div for thickness
	Hoop	0.27 - 0.53 mm/div
	Radial	0.27 - 0.44 mm/div
Analysis scheme		3D
Cell type		Hexahedron

As the turbulent flow was neglected, the pressure P_1 and the flow velocity u_m at the nozzle exits should approximately have a linear relationship. Examples are shown for the stroke S of 3.8 and 10.2 mm in Figure 6, assuming the uplift Δz is 10 μm . The curve obtained by Darcy-Weisbach equation, which is shown in Figure 4, is also drawn. The intersection points between the curve and the linear lines are the solution satisfying both of the nozzle and water film properties, for the each stroke. When the stroke S is 3.8 mm, the flow velocity u_m at the solution is over 100 $\text{m}\cdot\text{s}^{-1}$ as there is a gaping space between the material and the die as shown in Figure 3(a). On the other hand, when S is 10.2 mm, the flow velocity u_m is little as the nozzle is completely covered by the material as shown in Figure 3(b).

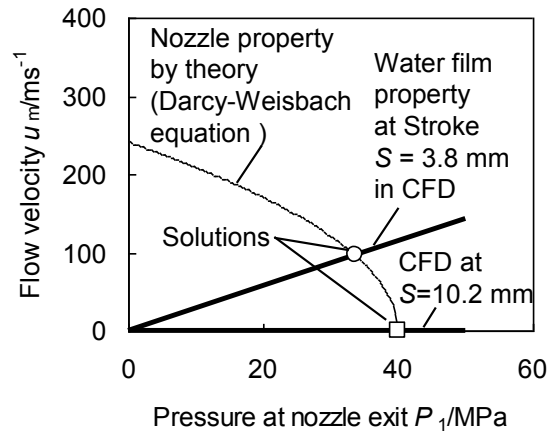


Figure 6: Decision of pressure and flow at the nozzle exit from theory of nozzle (Darcy-Weisbach equation) and CFD for water film (uplift Δz is assumed to be $10 \mu\text{m}$)

4 NUMERICAL RESULTS

As the uplift of material above the die upper surface Δz is unknown, a series of numerical analyses was carried out according to the progress of deep drawing, assuming Δz as 10, 15 and $20 \mu\text{m}$. Figure 7 shows the total force from fluid film on lower surface of the material F_z , by integrating pressure by area in vertical direction in CFD. The die load F_D , which is equal to the addition of the punch load and blank holding force, is also drawn as a result of the FEM on deformation. When the uplift Δz was 15 or $20 \mu\text{m}$, the force from water film F_z was less than the die load F_D . On the other hand, when Δz is $10 \mu\text{m}$, F_z is larger than or equal to F_D for the stroke S of 9 - 16 mm. Therefore, it would be supposed that the blank should be uplifted above the die surface by about $10 \mu\text{m}$ except the early and end stages of deep drawing.

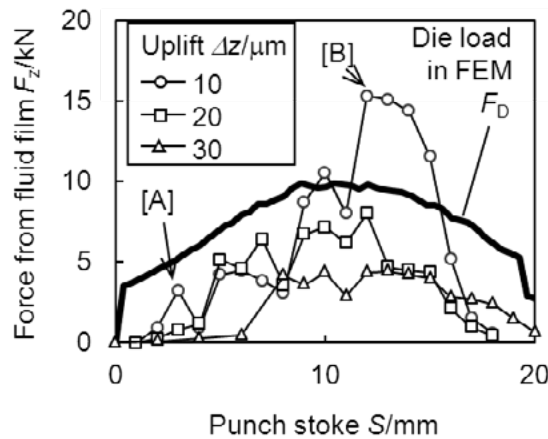


Figure 7: Total force from water film on lower surface of material

Figure 8 shows the pressure distributions obtained by CFD at the stroke S of 4 and 12 mm corresponding to the condition denoted by [A] and [B] in Figure 7, respectively. When the stroke S is 4 mm, the pressure is very low at the water film because of the pressure drop at the nozzles, because a large gaping space exists between the blank and the die. When the stroke S is 12 mm, a high pressure region widely appeared leading to the large force as denoted by [B] in Figure 7. Figures 7 and 8 would explain the mechanism which caused dimples at the early stage of deep drawing which was shown in Figure 2 and the efficiency of the proposed deep drawing. At the early stage, e.g. $S = 4$ mm, a large velocity volume of high pressured water collided against the material surface. On the other hand, in the middle of deep drawing, the velocity volume of pressured water was properly suppressed and a high pressured region widely appeared to lift up the material against the die surface.

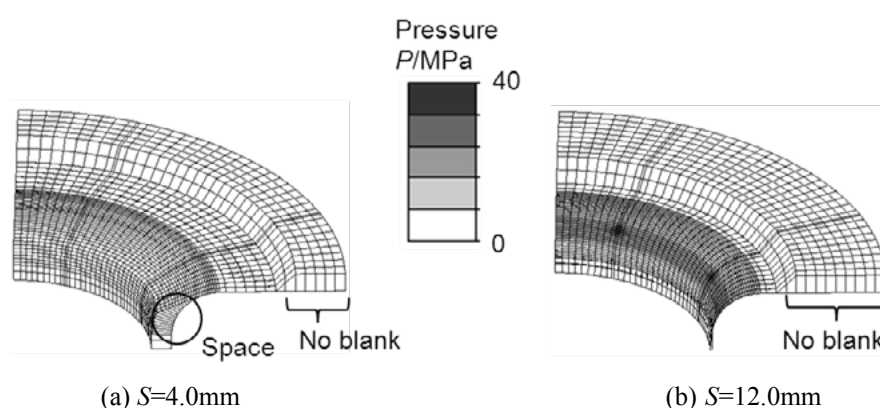


Figure 8: Pressure distribution obtained by CFD

12 CONCLUSIONS

- A numerical method was introduced for the evaluation of lubrication behavior of a deep drawing method with high-pressured water jet.
- In the numerical method, theory of fluid dynamics was used for evaluation of fluid characteristics inside the nozzle, while the Reynolds' equation was assumed for the thin film of fluid between the die and blank.
- The data of blank deformation in FEM was considered for the determination of the thickness distribution of the fluid film. The characteristics of the water were evaluated by the composed numerical method.
- As a result, it was numerically revealed that the pressure varies depending on the position and the stroke significantly. In particular, in the middle of process, the fluid flow worked well to lift up the material against the die surface.

REFERENCES

- [1] Nakano, M., Ueki, H., Utsunomiya, H. Effects of tandem pass drawing conditions on surface gloss of Ni-plated steel wire, *J. of Japan Society of Technology for Plasticity*

- (2011) **52**-602:365-369, in Japanese.
- [2] Yamashita, M., Gotoh, M., Hayashi, M. Development of lubricant for deep-drawing of pure titanium sheet, *J. of Japan Society of Technology for Plasticity* (2006) **47**-544:389-393, in Japanese.
- [3] Nakagawa, T., Nakamura, K., Amino, H. Various applications of hydraulic counter pressure deep drawing, *J. Mater. Process. Technol.* (1997) **71**-Issue 1:160-167.
- [4] Zhang, S.H., Lang, L.H., Kang, D.C., Dankert, J., Nielsen, K.B. Hydromechanical deep-drawing of aluminum parabolic work pieces -experiments and numerical simulation, *Int. J. Mach. Tool. & Manu* (2000) **40**:1479-1492.
- [5] Murata, M., Kuboki, T. Deep drawing of 1050 aluminum sheets using high pressure jet water as lubricant, *J. Jpn. Inst. Light Metals* (2006) **56**-9:469-473, in Japanese.
- [6] Kuboki, T., Saito, H., Tanaka, Y., Murata, M., Matsui, K., Tsubokura, M. Lubrication characteristics of deep drawing with high-pressured water jet, *Metal forming* (2012) Krakow, 355-358.
- [7] de Souza Neto, E.A., Peric, D., Dutko, M., Owen, D.R.J. Design of simple low order finite elements for large strain analysis of nearly incompressible solids, *Int. J. Solids Struct.* (1996) **33**-20-22:3277-3296.
- [8] Swamee, P.K., Jain, A.K. Explicit equations for pipe-flow problems, *J. of the hydraulics division* (ASCE) (1976) **105**-5:657-664.
- [9] Manning, F.S., Thompson, R.E. *Oilfield processing of petroleum: natural gas* (1991) 1:293, PennWell Books.
- [10] Dowson, D., Higginson, G.R. *Elasto-hydrodynamic lubrication*, SI ed. (1977) 22-29, Pergamon press.

ACKNOWLEDGEMENT

The present paper benefited partially through association with researchers in Japan and the UK. The CFD part was propelled thanks to Professor Emeritus Dr. Kuroda at the University of Electro-communications and Dr. Piao in Firmflow Co., Ltd in Japan. The FEM part was expedited thanks to Drs Rance, Armstrong, Dutko and other members in Rockfield Software Ltd. Wales, UK. This research was also supported by Grant-in-Aid for Scientific Research (Kaken) from JSPS, No. 22360303.